Available online at www.sciencedirect.com
ScienceDirect
Journal of Nuclear Materials 374 (2008) 54–60
journal of nuclear materials
www.elsevier.com/locate/jnucmat

TEM investigation of long-term annealed highly irradiated beryllium

W. Van Renterghem *, A. Leenaers, S. Van denBerghe

SCK·CEN, Nuclear Materials Science Institute, Boeretang 200, 2400 Mol, Belgium

Received 19 February 2007; accepted 11 July 2007

Abstract

Beryllium, irradiated at around 50 °C for 15 years up to a fast neutron fluence (>1 MeV) of 4.67×10^{22} n cm^{-2}, was annealed at temperatures of 500, 750, 825 and 900 °C. In a previous study, the influence of the annealing temperature and time on the He content and the microstructure was investigated with optical and scanning electron microscopy. To complement the observations made, transmission electron microscopy measurements on the same set of specimens were conducted to determine the helium behaviour at nanometer scale. It was found that the as-irradiated material is heavily stressed and contains many dislocation loops. In the samples annealed at 500 and 750 °C, these dislocation loops disappeared and a large number of small faceted bubbles have formed inside the grains. Close to grain boundaries, a bubble-free area was observed. Annealing at 825 and 900 °C results in the complete removal of all small bubbles, and the local defect structure reverts back to the one of the un-irradiated material.

1. Introduction

In the design of a thermonuclear fusion reactor, beryllium is a candidate material for constructing the plasma facing material and the neutron multiplier [1]. Hereto, the behaviour of this material under high neutron fluences and high temperatures is being investigated. The production and diffusion of gases like helium and tritium is an important issue. High quantities of these gases are produced as a result of the neutron multiplication reaction ^{9}Be(n,2n)2^{4}He and the reaction chain ^{9}Be(n,α)^{6}He(β^{-})^{6}Li(n,α)^{3}H.

The diffusion of ^{4}He and ^{3}H atoms as created by neutron irradiation of beryllium has been discussed in the literature [2–5]. The solubility of both elements in beryllium is very low and they will easily precipitate into small gas bubbles. If irradiated at low temperature (50–150 °C), the swelling is limited [2], but the beryllium exhibits substantial hardening and embrittlement. The He atoms are mostly trapped at vacant Be lattice sites [6] or in the vicinity of dislocations [5]. The dislocations are pinned by the gas atoms, causing the hardening and embrittlement. At higher temperatures, the He atoms and vacancies are mobile and internal gas-filled bubbles and voids are formed. With increasing temperature, the gas bubbles grow and eventually coalesce, inducing important swelling of the material, which limits its lifetime in the reactor.

In a previous publication by Leenaers et al. [7] on the same material as investigated here, the retained helium content and specimen density were measured and the bubble formation was visualized with optical microscopy (OM) and scanning electron microscopy (SEM). It was found that annealing of the samples at 500 °C causes the gas atoms to migrate to the grain boundaries and precipitate into small bubbles. At 750 °C, the observed intergranular bubbles have grown and started to coalesce. Also intragranular bubbles are formed at this annealing temperature. At an annealing temperature of 900 °C even larger bubbles have grown at the grain boundaries by coalescence and they started to interlink. Retained ^{4}He measurements showed that the latter samples have experienced a complete gas release during annealing and a saturation of the swelling was observed in the density measurements for an annealing temperature above 750 °C.

* Corresponding author. Tel.: +32 14 333098; fax: +32 14 321216.
E-mail address: wvrenter@sckcen.be (W. Van Renterghem).

0022-3115/$ - see front matter © 2007 Elsevier B.V. All rights reserved.
doi:10.1016/j.jnucmat.2007.07.007

It was concluded that the changes observed in the microstructure of the annealed beryllium samples are mainly influenced by the annealing temperature. Some minor effect of the annealing time was noticed at high annealing temperature (900 °C). Image analysis on the microscopy images of the sample annealed at 900 °C for 2160 h showed that there is still a microstructural evolution in the material, even after complete gas release. It was assumed that sintering causes nanometer-sized voids to migrate to either the grain boundary where they coalesce with the intergranular bubbles or to the existing large intragranular bubbles, resulting in the observed increase of the visible porosity without additional density changes.

OM and SEM allow only the observation of the larger bubble population (>100 nm), while the initial stages of the bubble formation cannot be resolved using these techniques. The discrepancy between the theoretically calculated swelling and the measured porosity indicates that part of the gas cannot be accounted for in the observations. Therefore, transmission electron microscopy (TEM) was applied on the same specimens as used in the previous study, to evaluate the bubble formation on nanometer scale and the effect of annealing temperature and time on it.

2. Experimental

The specimens and annealing parameters are fully described in the paper of Leenaers et al. [7]. Only the most important features are repeated here. The composition of the material is given in Table 1. It is an S-200-E grade Be, manufactured by vacuum hot pressing of impact-attritioned Be powder of at least 100 mesh. It was part of the second matrix of the Materials Testing Reactor BR2 at SCK·CEN and was in the reactor for 15 years before it was replaced in 1995. In this period, the matrix was exposed to a fast fission neutron fluence ($E > 1$ MeV) of 4.67×10^{22} n cm^{-2} [8] at a temperature of around 50 °C. The amount of He produced in this period is about 2.2 at.% which is comparable to the amount of He expected in a typical Be fusion reactor blanket at the end of its life. Also a significant amount of ^{3}H, approximately 0.2 at.%, is produced [9]. Because of the irradiation conditions, the amount of ^{3}H is much higher than expected to be generated in a fusion reactor. However, after 11 years out of pile, about half of the produced ^{3}H will have decayed into ^{3}He. It should be noted that with TEM, no distinction can be made between ^{4}He and ^{3}H atoms. In the literature, it is reported that ^{4}He and ^{3}H behave similarly, but the gas precipitation rate for ^{3}H is lower than for ^{4}He [5]. As a consequence, the ^{3}H migrates faster towards the grain boundaries and a higher fraction is released at lower temperature [10]. The gas in the bubbles will be a mixture of mainly ^{4}He atoms and a small amount of ^{3}H. Therefore, in the remainder of the paper, only the ^{4}He atoms will be mentioned, but it should be remembered that the gas also contains ^{3}H and ^{3}He atoms.

To simulate the behaviour of the ^{4}He in a fusion reactor, the irradiated specimens have been annealed in a horizontal tube furnace (Adamel type M05HT) in a hot cell at temperatures of 500, 750, 825 and 900 °C for periods ranging between 50 h and 3 months. The annealing does not fully compensate for the differences in irradiation conditions, but a qualitative understanding of the ^{4}He behaviour can be obtained in this way.

The beryllium samples were mechanically polished to a thickness of about 100 μm after which 3 mm discs were punched out. The as-irradiated specimens broke into small pieces during punching indicating the brittleness of the material. The largest fragments were collected and glued on a golden grid with an aperture of 1 mm. All specimens were electrochemically polished using an electrolyte consisting of 25% H_2SO_4 and 75% methanol. The temperature was −18 °C and the applied voltage 20 V. The specimens were investigated using a JEOL 3010 microscope operating at 300 kV. Conventional bright field and dark field imaging was applied and the thickness of the specimen was measured using convergent beam electron diffraction patterns.

3. Results

3.1. The blank material and as-irradiated specimen

The blank, un-irradiated material with the same composition and manufacturing process as the other specimens was investigated for comparative reasons. A typical image of the microstructure is shown in Fig. 1(a). The analysis of the Burgers vector is not shown explicitly here, but it was determined that predominantly ⟨a⟩ type dislocations are present in this material.

Fig. 1(b) shows the microstructure of the as-irradiated material. The specimen was irradiated up to a fast neutron fluence of 4.67×10^{22} n cm^{-2} at low temperature, resulting in an accumulated He content of 2.2 at.%. It can be calculated and measured that the swelling is limited. No bubbles can be found in the TEM images. These observations are in agreement with literature data, where bubble formation was not observed in specimens irradiated at low temperature before annealing [11,12]. Instead

Table 1
Chemical composition of the beryllium specimens in wt% as supplied by the manufacturer

Be	BeO	Fe	C	Al	Mg	Si	Other metallic elements
>98	<2.0	<0.18	<0.15	<0.15	<0.08	<0.08	<0.04 each

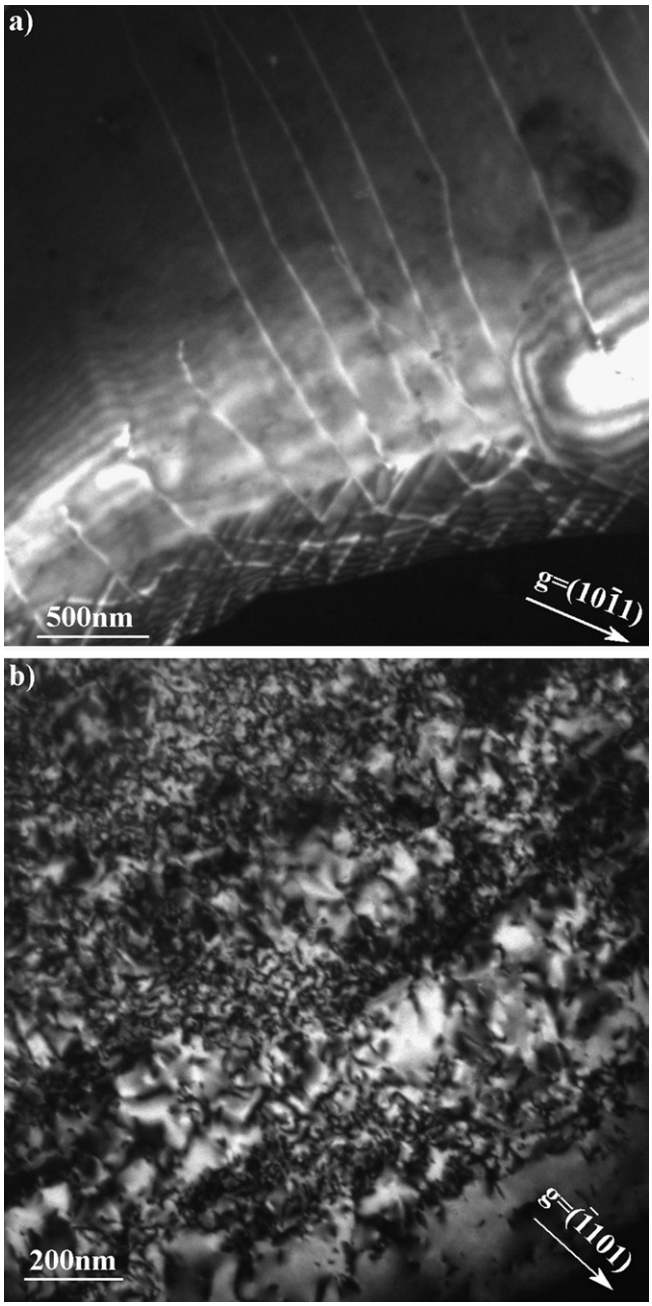

Fig. 1. (a) Dark-field image showing the dislocation structure of the un-irradiated material and (b) dark-field image of the irradiated material before annealing. A stray contrast, indicating a large amount stress, can be observed. In between the stray contrast small radiation induced dislocation loops can be observed.

of bubbles, a stray contrast is present throughout the specimen (Fig. 1(b)). This contrast cannot be identified as a single defect, but it indicates that a large amount of stress is present in the material. The presence of internal stress in irradiated Be is reported in the literature [6,13]. Because of the smaller radius of He compared to Be, the trapped atoms are not expected to introduce large lattice distortions. The observed stress is therefore probably resulting from small gas clusters which are too small to be visualised by TEM.

In between the stray contrast, also radiation induced dislocation loops are found. The type of loops was not determined in this experiment, but the average size of the loops and the loop density were measured to be 15 nm and 4×10^{21} m^{-3}, respectively. These values are comparable to the results of Chakin and Ostrovsky [11] under similar irradiation conditions, but on irradiated beryllium with lower helium content.

3.2. The specimens annealed at 500 °C

After the annealing at 500 °C for 50 h, the microstructure of the specimens has changed significantly. Throughout the centre of the Be grains, a large amount of bubbles is formed, but there seems to be no apparent relation with the pre-existing dislocations. The shape of the bubbles is that of a hexagonal prism with the basal plane parallel to the (0002) basal plane of the Be lattice. The TEM images (Fig. 2(a)) show the projected shape of the bubbles, but it is the combination of images recorded in different orientations that leads to the observation that the bubbles are indeed hexagonal prisms. The average edge length in the basal plane is 8.6 nm and the average prism height is 12.3 nm. The bubble density equals 2.2×10^{22} m^{-3}.

Close to the grain boundaries (Fig. 2(b)), a region depleted of bubbles is found. The width of this region differs from grain boundary to grain boundary, but in some cases it was more than 1 μm broad. Within the bubble-free region, ⟨a⟩-type dislocations are found, similar to the dislocations in the un-irradiated specimen. An occasional spherical bubble is still observed in this area, but not in the large amount as in the centre of the grain. No radiation induced dislocation loops remain, neither in the area containing bubbles, nor in the region close to the grain boundaries.

On the grain boundary, larger bubbles of a few hundred nm long are observed. The edges of the bubble still correspond with crystallographic planes of the Be matrix, but because both halves of the bubble lie in two differently oriented grains, their shape is more irregular.

To investigate the effect of the annealing time, two additional specimens, which were annealed at 500 °C for 200 h and 2106 h, were analysed (see Fig. 3). Similar results were obtained on both samples. Close to the grain boundary, again a defect free region is found, but it is smaller than in the specimen annealed for 50 h. Away from the boundary, a large amount of bubbles is again present. Compared to the 50 h annealed specimen, the bubbles are more rounded, but they still have the shape of a hexagonal prism. The size of the bubbles has not changed significantly. The average edge lengths in the *a*- and *c*-directions are 6.9 nm and 10.4 nm and 6.9 nm and 11.0 nm in the specimens annealed for 200 and 2106 h, respectively. The TEM-investigation confirms the results of Leenaers et al. [7] that a longer annealing time at 500 °C has only a limited effect on the gas behaviour.

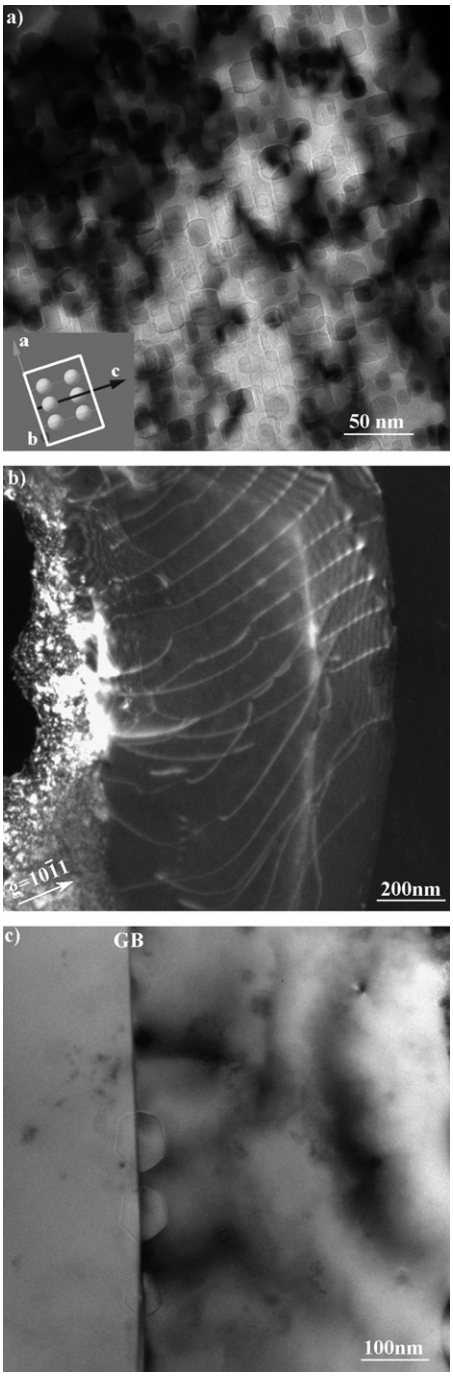

Fig. 2. Microstructure of Be annealed at 500 °C. (a) Projected shape of the He bubbles. The inset shows a magnified Be unit cell, projected on the image plane to indicate the relevant directions. (b) Dark-field image showing the area close to a grain boundary which is depleted of He bubbles. (c) Bright-field image showing He bubbles on the grain boundary.

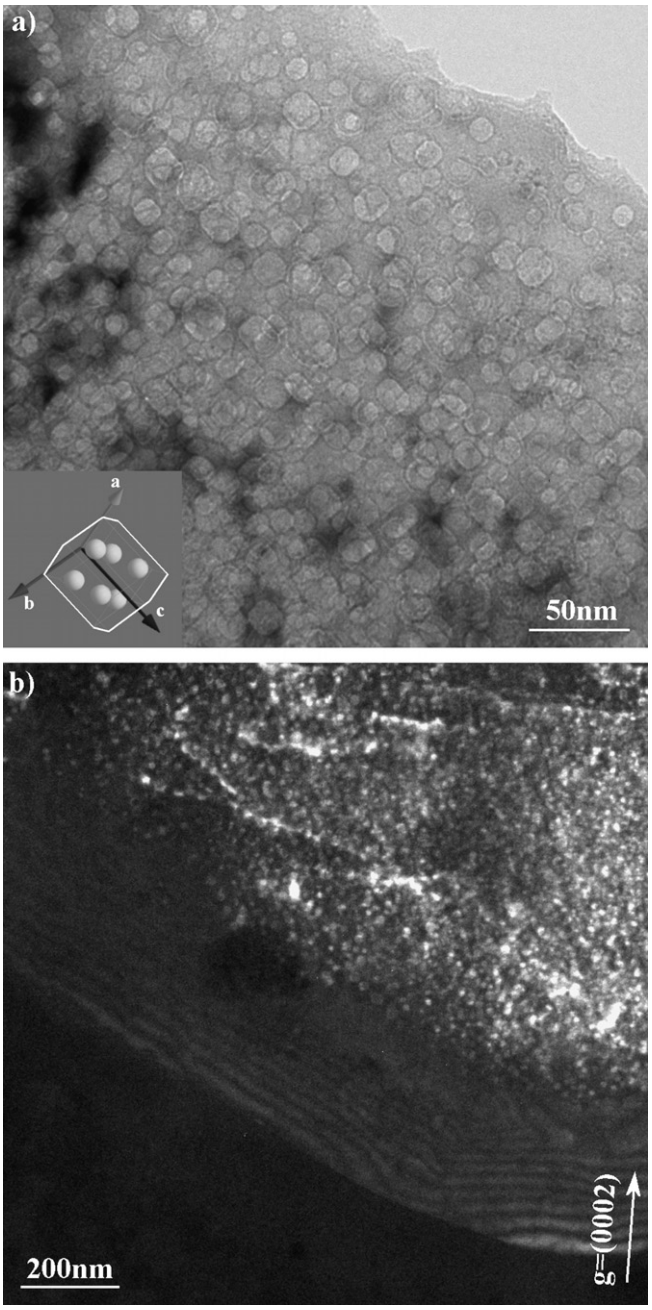

Fig. 3. (a) Bright-field image showing the ^{4}He bubbles in the specimen annealed at 500 °C for 200 h. The inset shows the projected image of the Be unit cell and the relevant directions. (b) Dark-field image of the specimen annealed for 2106 h showing the defect free area close to the grain boundary.

3.3. The specimens annealed at 750 °C

The microstructure of the specimen annealed at 750 °C for 50 h, is very similar to the specimen annealed at 500 °C. In the centre of the grain (Fig. 4(a)), a large amount of bubbles with a hexagonal prism shape has been observed. The average size of the bubbles has not changed significantly. The edge lengths are 8.4 nm in the basal plane and 11 nm in the *c*-direction. Also the bubble density did not change at the higher annealing temperature. It was measured to be 2.3×10^{22} m^{-3}. Close to the grain boundary, a defect free region is observed again (Fig. 4(b)), which sometimes reaches a width of 1.5 μm.

The SEM measurements [7] report the start of the coalescence of the bubbles at the grain boundaries and the formation of large intragranular bubbles. The size of these bubbles is of the order of a few micrometers, which for

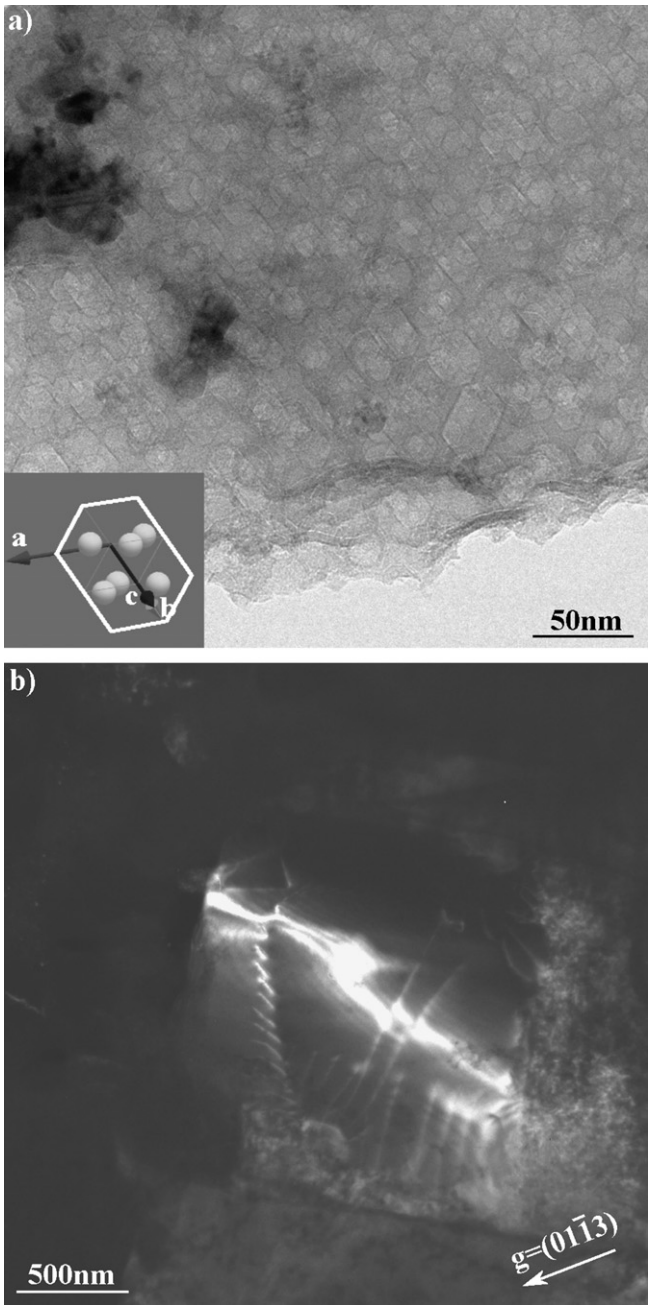

Fig. 4. (a) Bright-field image showing the He bubbles in the specimen annealed at 750 °C. The inset shows the projection of the unit cell and all relevant directions. (b) Dark-field image showing the defect free area adjacent to a grain boundary.

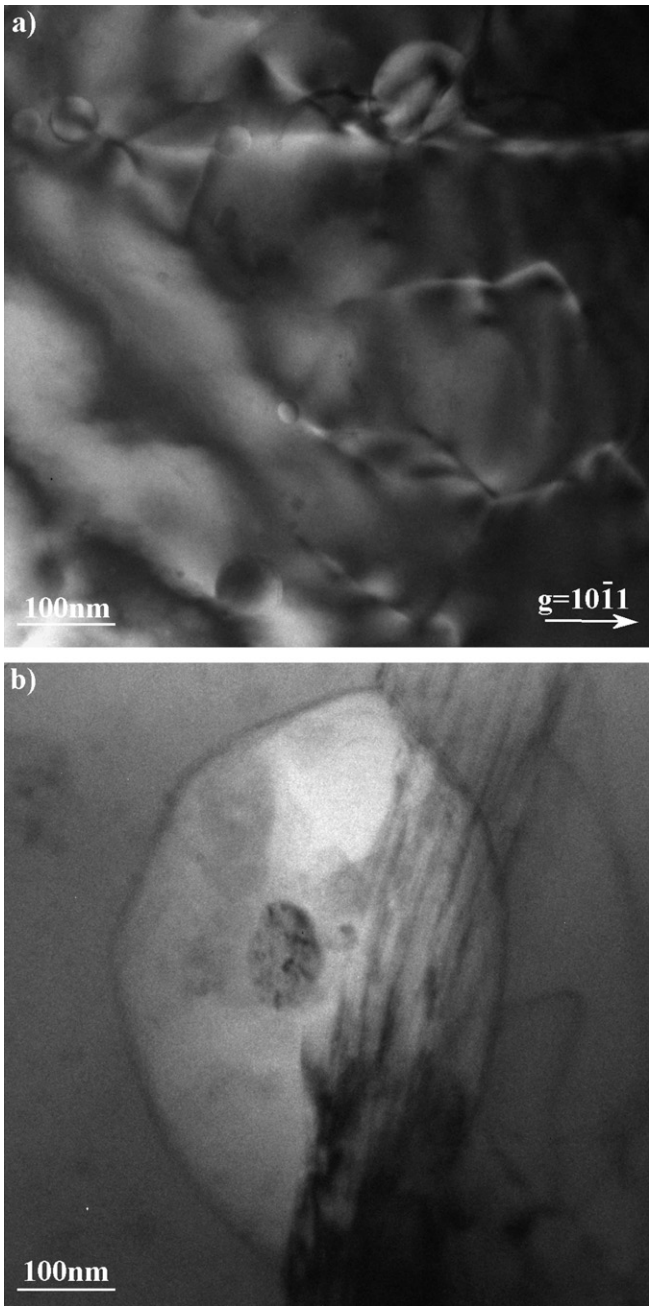

Fig. 5. (a) Dark-field image showing the line dislocations and residual ^{4}He bubbles in the specimen annealed at 825 °C. (b) ^{4}He bubble at the grain boundary.

TEM is too large to distinguish from a hole created during the electrochemical polishing.

3.4. The specimens annealed at 825 °C and 900 °C

Annealing at even higher temperatures does influence the microstructure significantly as shown in Fig. 5 for the specimen annealed at 825 °C for 50 h. The faceted bubbles are no longer present in the grain interiors and only a limited number of isolated round bubbles with different diameters are found in this specimen. In Fig. 5(a), the smallest bubble has a diameter of 6 nm, while the diameter of the largest bubble is 105 nm. The larger bubbles at grain boundaries are still present, but contrary to what is found after annealing at 500 °C, the edges of these bubbles are rounded off and they have a lenticular shape (Fig. 5(b)), indicating interlinking of bubbles.

As expected, the radiation induced dislocation loops, which were already annealed out at 500 °C, have not been found back in this specimen. The remaining defect structure is very similar to the defect structure of Be before

irradiation (Fig. 1(a)) in the sense that mostly regular line dislocations are found.

Using different two-beam conditions, the Burgers vector of the dislocations was determined, and by tilting the specimen, the direction of the dislocations was found. It was established that the majority of the dislocations are ⟨a⟩ type dislocations, but also ⟨c⟩ type dislocations were found. For most dislocations, the Burgers vector is parallel to their direction, which means that they are screw dislocations.

The results for the specimen annealed at 900 °C for 50 h are comparable to the 825 °C annealed specimen. No bubbles were observed in the centre of the grain, no irradiation induced dislocation loops were found, and the defect structure is again very similar to the non-irradiated specimen.

4. Discussion

The TEM measurements of the irradiated and annealed beryllium specimens reported in this paper provide additional information on the helium behaviour. During irradiation at low temperature, a large amount of gas is formed. Most of the helium atoms are trapped at vacant Be sites, which are formed during neutron irradiation, but also some gas clusters are formed which are the nucleation sites for internal bubble formation. The gas clusters cannot be observed in TEM directly, but their presence can be assumed because of the large amount of stray contrast which will be induced by lattice distortions around the clusters. For the growth of the bubbles, the trapped He atoms need to diffuse towards the clusters, but also the surrounding matrix atoms have to be displaced to provide sufficient space for the gas [3]. This will occur only at temperatures where a sufficient amount of vacancies can flow towards the ^{4}He atoms.

After a heat treatment at 500 °C, the agglomeration of ^{4}He into bubbles is observed. At this temperature, the mobility of the vacancies and He-vacancy clusters is sufficient to allow the nucleation of bubbles. Near grain boundaries, a bubble-free area is observed, as also reported by Rich et al. [2]. One explanation could be that the vacancies formed in that area diffused towards the grain boundary, preventing bubble formation. However, also the strain contrast is no longer observed there, which indicates that also the gas atoms formed in that region have diffused towards the grain boundary forming the larger bubbles observed in Fig. 2(c).

The observed bubbles are faceted and have the shape of hexagonal prisms. In general, a bubble will try to minimize the elastic strain energy. Therefore, an overpressurised bubble will tend to become spherical. However, within a matrix, the total free energy of the system has to be reduced. Goodhew [14] has shown that all bubbles of which the growth is limited by collecting of vacancies will tend to become faceted onto low energy faces. In crystals with an hcp crystal structure, the low energy faces are the (0 0 0 1) basal plane and the $10\bar{1}0$ prism planes. This is in agreement with the observations described in this paper.

Furthermore, it can be expected that the size of the bubbles grows for longer annealing times and higher temperatures [15]. It was shown that the modal bubble radius at constant gas content increases with annealing time t according to the relationship

$$r^n \propto DT^m t \tag{1}$$

with r the bubble radius, D the diffusion coefficient, and T the annealing temperature. The values of n and m depend on the exact bubble growth mechanism. For growth by Ostwald ripening, the exponent n equals 2, while for migration and coalescence growth, the exponent varies between 3 and 6, depending on the particular diffusion mechanism. However, when faceted bubbles are formed, the nucleation of steps on the bubble surfaces becomes the rate controlling mechanism, which is called ledge nucleation. Eq. (1) is no longer obeyed and the growth rate decreases steadily with size.

The results presented here do not show a change in the size of the bubbles in the interior of the grain with longer annealing times or higher temperatures. This could be due to the fact the shortest annealing time is 50 h and the bubbles are already quite large. The larger the facet length, the lower the bubble diffusion coefficient and the lower the bubble growth rate. The investigation of specimens annealed for a longer time, showed that no coalescence of bubbles occurred and that the bubbles are immobile at 500 °C.

Furthermore, it was observed that the radiation-induced dislocation loops were annealed out in these specimens. These loops were formed by the agglomeration of either interstitial Be atoms or vacancies. Their annealing suggests that all vacancies formed diffused to the grain boundaries or to the faceted He bubbles. Already after 50 h of annealing, no more vacancies are available for further bubble nucleation or growth.

The specimen annealed at 750 °C shows faceted bubbles in the grain interior of similar size and density as in the specimen annealed at 500 °C but the main difference is that the bubble-free area next to a grain boundary has on average slightly enlarged. The SEM measurements [7] show a significant enlargement of the helium bubbles at the grain boundaries. At the same time, an increase in swelling is reported and a release of nearly 50% of the retained He content is measured. This observation suggests that because of the higher ^{4}He-vacancy cluster mobility at these temperatures, additional gas atoms have become available for bubble growth at the grain boundary. Additionally, it cannot be excluded that some of the bubbles, already formed at the grain boundary, have coalesced to form larger bubbles. The fact that the faceted bubbles do not grow despite the higher helium-vacancy cluster mobility, might indicate that ledge nucleation is indeed the rate controlling mechanism. It also shows that the faceted bubbles are not mobile at 750 °C.

The specimens annealed at 825 °C and 900 °C do no contain faceted bubbles anymore. This annealing tempera-

ture is sufficiently high for the bubbles themselves to become mobile and to migrate towards the grain boundaries. The SEM investigations have shown that, at these temperatures, the grain boundary bubbles become interlinked and form channels for gas release and most of it has been released. The swelling saturates at these annealing temperatures, which suggests that no additional helium is added to the bubbles. The growth of the bubbles observed with OM and SEM is therefore only the result of the diffusion and absorption of the small faceted bubbles and the coalescence of the larger grain boundary bubbles, which do not change the total volume.

5. Conclusions

The helium and tritium gas bubble formation in highly irradiated beryllium was investigated with TEM as a function of annealing temperature.

Before annealing, the irradiated material shows a large number of irradiation induced dislocation loops but no helium bubbles. The average loop size is 15 nm and the loop density equals 4×10^{21} m^{-3}. There is a high amount of stress present in these specimens, which is related to the presence of small gas clusters, which are too small to be visible in TEM images.

After anneals at temperatures of 500 and 750 °C, a large amount of bubbles with a hexagonal prism shape is observed in the interior of the Be grains. The average edge lengths are comparable for both annealing temperatures and also an increase of the annealing time does not have a significant effect on the bubble size. The edge lengths lie between 6.9 and 8.6 nm in the *a*-direction and between 10.2 and 12.3 nm in the *c*-direction. The area close to the grain boundary is found to be defect free, except for some ⟨a⟩ type line dislocations which are also found in the unirradiated material. It is argued that the gas atoms from this area have diffused to the grain boundary to form larger bubbles. The irradiation induced defects are annealed out of the specimen at these temperatures.

Annealing at 825 and 900 °C results in the removal of virtually all small ^{4}He bubbles observed in the grain interior. Only the line dislocations, also present in the specimen before irradiation, are observed. The majority of the dislocations are ⟨a⟩-type, but the presence of a small amount of ⟨c⟩-type dislocations was reported as well.

Regarding the helium mobility, the experiments show that at 500 °C the ^{4}He atoms are sufficiently mobile to create bubbles. Small faceted bubbles are formed, which themselves are still sessile. The mobility of the gas atoms increases with higher temperature and the saturation of the swelling at 750 °C suggest that all ^{4}He is present in bubbles. The small faceted bubbles are mobile above 825 °C and contribute to the further growing of the large grain boundary bubbles, but this does not induce a further significant swelling of the beryllium.

References

[1] F. Elio, K. Ioki, P. Barabaschi, L. Bruno, A. Cardella, M. Hechler, T. Kodama, A. Lodato, D. Loesser, D. Lousteau, N. Miki, K. Mohri, R. Parker, R. Raffray, D. Williamson, M. Yamada, W. Daenner, R. Mattas, Y. Strebkov, H. Takatsu, Fusion Eng. Des. 46 (1999) 159.
[2] J.B. Rich, G.B. Redding, R.S. Barnes, J. Nucl. Mater. 1 (1959) 96.
[3] R.S. Barnes, J. Nucl. Mater. 11 (1964) 135.
[4] J.M. Beeston, Gas release and compression properties in beryllium irradiated at 600 and 750 °C, in: Effects of Radiation on Structural MetalsASTM STP, vol. 426, Am. Soc. Testing Mats., Philadelphia, 1967, p. 135.
[5] E. Rabaglino, Helium and tritium in neutron-irradiated beryllium, Forschungszentrum Karlsruhe Report, FZKA 6939, 2004.
[6] J.B. Mitchell, J. Fusion Energy 5 (1986) 327.
[7] A. Leenaers, G. Verpoucke, A. Pellettieri, L. Sannen, S. Van den Berghe, J. Nucl. Mater., in press, doi:10.1016/j.jnucmat.2007.03.214.
[8] L. Sannen, C. De Raedt, F. Moons, Y. Yao, Fusion Eng. Des. 29 (1995) 470.
[9] Ch. M. De Raedt, L.F. Sannen, P.J. Vanmechelen, B.M. Oliver, H. Werle, in: Ninth International Symposium on Reactor Dosimetry, September 2–6, Prague, Czech Republic, 1996, p. 4.
[10] I.B. Kuprianov, V.A. Gorokhov, V.V. Vlasov, Fusion Engineering, 1995 SOFE'95, "Seeking a New Energy Era", 16th IEEE/NPSS Symposium, vol. 2, 1995, p. 948.
[11] V.P. Chakin, Z. Ye Ostrovsky, J. Nucl. Mater. 307–311 (2002) 657.
[12] D.V. Andreev, V.N. Bespalov, A. Ju. Birjukov, B.A. Gurovich, P.A. Platonov, J. Nucl. Mater. 233–237 (1996) 880.
[13] V.P. Chakin, V.A. Kazakov, R.R. Melder, Yu.D. Goncharenko, I.B. Kupriyanov, J. Nucl. Mater. 307–311 (2002) 647.
[14] P.J. Goodhew, J. Nucl. Mater. 98 (1981) 221.
[15] T.R. Armstrong, P.J. Goodhew, Radiat. Effect 78 (1983) 35.